OPERATIONAL WIND-WAVE FORECASTING SYSTEM FOR THE GULF OF MEXICO

José Antonio Salinas Prieto[1]
Roberto Padilla Hernández[2]
Fernando Oropeza Rosales[1]
René Lobato Sánchez[1]

1 Instituto Mexicano de Tecnología del Agua
Paseo Cuauhnauac 8532, Col. Progreso, CP 62550
Jiutepec, Morelos
Email: jsalinas@tlaloc.imta.mx

2 Universidad Autónoma de Tamaulipas
Centro Universitario Tampico-Madero
Tampico, Tamaulipas. México
Email: rpadillah@uat.edu.mx

1. INTRODUCTION

The forecasting of high waves associated to extreme atmospheric events, such as cold fronts and hurricanes in the Gulf of Mexico (GoM) has become an important issue due to lost of lives, severe damage to human activities and societal infrastructure. Every year the GoM is the scene, on average, of 25 tropical storms (between June and October) and 40 cold fronts (between November and April). Moreover wind-waves play an important roll in ocean-atmospheric interactions, intensifying the properties exchange among these two systems, through aerosol, mainly during tropical storms and hurricane situations. The intensification is up to two orders of magnitude larger due to the presence of deep water wave breaking. During a hurricane situation, the deep-water wave breaking is a feedback mechanism for the hurricane, affecting the intensification and, although in smaller degree, also its trajectory.

That is why wind-wave simulation and forecasting have an increasing demand of diverse social, economic and scientific sectors, which require planning activities to short, medium and long terms

Wind-waves along with wind and currents are responsible for the changes in the coastal morphology: The coastal line will change in function of sediment and energy budget, this energy comes mainly from the wind-waves, during the shoaling process the energy wave dissipation generates turbulence placing sediment in suspension, which can be transported like load, saltation or drags, or a combination of these forms. During extreme meteorological events, like hurricanes, these processes can modify the coastal configuration visibly. For example the case of Beaches of Cancun, in the Mexican Caribbean; during the passage of the Wilma Hurricane, in 2005, Cancun suffered a severe erosion, and the beach recovery implied great investments and technology, for that reason the planning and suitable design of the coastal infrastructure taking into account the surge, are fundamental. The wave forecast is useful in the decision making to close or open the ports to navigation. Despite the high costs that imply the instrumentation, their positioning

and maintenance, the systematic measurement of waves is very useful. In Mexico, the budget of operative research centers is insufficient for this task, being important the use of alternative and complementary forms of investigation, like the numerical modelling.
The numerical modelling, with its limitations, has become the best tool for wave forecast, but it must be considered a good approach, their precisions depends on the knowledge of the phenomenon, the numerical technique and the user experience, as well as of the quality of wind data used to force the wave model. There has been an intense use of atmosphere and ocean numerical models, in recent years due to the technological advance in high performance computing devices their capacity of storage and low of costs. Thus, in the last 20 years the numerical modelling of the atmosphere became a tool incorporated to the operational community, since in its origins was confined for the scientific one. Particularly, in Mexico the wave models have not been use in an operational way.
For the operational wave forecasting system presented in this paper, the Operational wind-wave forecasting system (POMA according to its Spanish initials), three modern widely-used models are used: (a) MM5 model (Atmospheric model, NCAR, Dudhia, J., 1993), (b) WAM (WAMDI Group, 1988), version WAM-PROMISE (hereafter denoted WAM) from Monbaliu et al. (2000), which is a modified version of WAM Cycle 4, and (c) SWAN version 40.20 (Booij et al., 1999),. SWAN was originally developed for high resolution coastal applications. WAM is suitable for global, regional basin-scale and shelf-scale applications, the version implemented in this study has several features that make it efficient in shallow water and high resolution applications. Model validation is based on data from buoys owned by the NDBC (National Data Buoy Center).

Section 2 presents the methodology to set up the numerical models, section 3 presents an overview of atmospheric and wave models. Section 4 describes the data used in this study, the study cases are described and the wave model validation is presented. Conclusions are presented in section 5.

2. METHODOLOGY

The implementation of waves and atmospheric numerical models was made in several steps:

a) Implementation of MM5 model (NCAR: National Center for Atmospheric Research, EU).
b) Implementation of WAM wave model (Max-Planck Institut fûr Meteorology, Germany, KNMI), to simulate the wave field in deep waters.
c) Implementation of SWAN wave model, nested in WAM, to simulate waves in intermediate and shallow waters.
d) Atmospheric-wave models one-way coupling
e) Validations of numerical simulations

The process is shown in Figure 1: the model MM5 provides the wind fields at 10 m height for both wave models (WAM simulates the swell in the Atlantic and provides the boundary conditions to SWAN, which simulates the wave fields in the Caribbean Sea and Gulf of Mexico). These results are evaluated using NDBC buoys. Etopo2 bathymetry, from the United States National Geophysical Data Center, at 2 minutes resolution, is used.

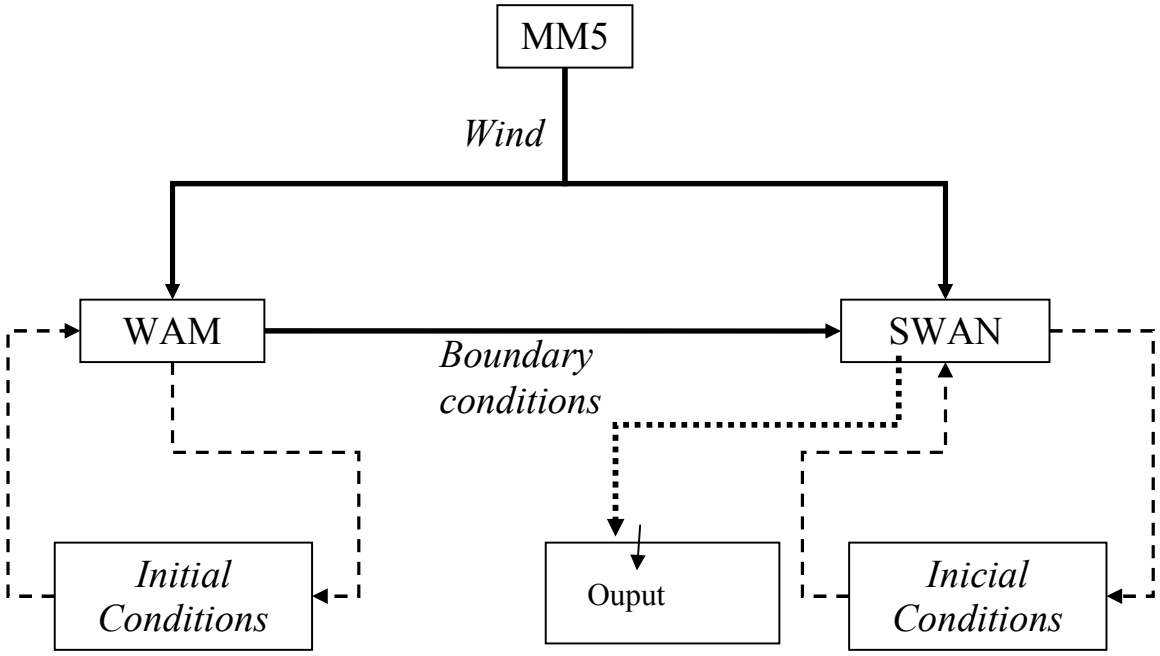

Figure 1. Flow diagram for wave forecast. The continuous arrows indicates the flow of information between models, dotted arrow indicates flow of information from a model to itself (as initial conditions in the re-initialization of runs), dotted heavy arrow output of final results.

The wave models are implemented on a system of two nested grids (Figs. 2 and 3). The spatial resolution increases from 1.0^{o} in the coarse grid to 0.1^{o} in the fine grid. The grid dimensions and resolutions are given in Table 1. WAM makes the coarse grid and SWAN is used on the fine grid, reading the boundary wave conditions from WAM with a 12 – minute time step which was shown numerically to give stable reliable simulations. The spectral range and resolution of the three models are given in Table 2, where f_{low}, f_{high}, n, Δf and $\Delta\theta$ are the lowest and highest frequencies, the number of points and the frequency and angular resolutions, respectively. For MM5 model the spatial resolution is 0.25 degrees.

MM5 produces 48 hours of wind forecast with a time resolution of 6 hours, those wind fields are transferred to the wave models to produce a wave forecast of 48 hours, at the hour 24, MM5 produces the next 48 hours, the wave models uses

the initial conditions at 24 hours and produces the next 48 hours of forecasting (from 24 to 72 hrs). The wave results to be presented in this paper are taken from the first 24 hours of every 48 hours time window.

3. MODELS DESCRIPTION

The selected models were develop by the international scientific community, and they have been tested under many environmental conditions, particularly the MM5 model have been tested and used operationally by the Mexican atmospheric community, this is not the case for WAM and SWAN. In México there is not an operational wave model system and this is our main concern, due to the fact that there is an increasing demand for a wave forecasting service.

3.1 THE ATMOSPHERIC MODEL MM5

The mesoscale model MM5 is a limited-area, nonhydrostatic model (which allows to be used at a few-kilometer scale), uses terrain-following sigma-coordinate (Dudhia, J., 1993). It is used to simulate mesoscale atmospheric events. The model contains pre- and post-processing modules, the modelling system is mostly written in Fortran, and has been developed at Penn State and NCAR as a community mesoscale model with contributions from users worldwide. This model includes a multiple-nest and multitasking capabilities. Terrestrial and isobaric meteorological data are horizontally interpolated from a latitude-longitude mesh to a variable high-resolution domain.
The model integrates the momentum and thermodynamics equations in the three components in sigma coordinate, using second order time-split leapfrog time scheme and second-order centered space scheme.
The sigma coordinate is defined by:

$$\sigma = \frac{p - p_t}{p_s - p_t} \qquad (1)$$

Where p is the pressure at different levels, pt is the top pressure, and ps is the surface pressure

The momentum equations in sigma coordinates in the flux form are:

$$\frac{\partial p^* u}{\partial t} = -m^2\left[\frac{\partial p^* uu/m}{\partial x} + \frac{\partial p^* vu/m}{\partial y}\right] - \frac{\partial p^* u\sigma}{\partial \sigma} - mp^*\left[\frac{RT}{\left(p^* + \frac{p_t}{\sigma}\right)}\frac{\partial p^*}{\partial x} + \frac{\partial \phi}{\partial x}\right] + p^* v(f+\gamma) + p^* w\left[r^{-1}2\Omega(\cos\phi)y - \frac{u}{a}\right] + FU \qquad (2)$$

(a) (b) (c) (d) (e) (f)

$$\frac{\partial p^* v}{\partial t} = -m^2\left[\frac{\partial p^* uv/m}{\partial x} + \frac{\partial p^* vv/m}{\partial y}\right] - \frac{\partial p^* v\sigma}{\partial \sigma} - mp^*\left[\frac{RT}{\left(p^* + \frac{p_t}{\sigma}\right)}\frac{\partial p^*}{\partial y} + \frac{\partial \phi}{\partial y}\right] + p^* u(f+\gamma) + p^* w\left[r^{-1}2\Omega(\cos\phi)x - \frac{v}{a}\right] + FV \tag{3}$$

For both equations: 2) and 3), the first term on the right side (a) represents the horizontal momentum flux divergence; the second term (b) the vertical momentum flux divergence, the third term (c) the thermodynamic effects and represent the inflow mass, (d) is the Coriolis parameter, the (e) term is the Coriolis horizontal component, and (f) the friction. The amounts m, r and γ are map factors defined respectively by:

$$m = \frac{sen\Psi_1}{sen\Psi}\left[\frac{\tan\frac{\Psi}{2}}{\tan\frac{\Psi_1}{2}}\right] \tag{4}$$

$$r = \frac{a}{n}sen\Psi_1\left[\frac{\tan\frac{\Psi}{2}}{\tan\frac{\Psi_1}{2}}\right]^n \tag{5}$$

$$\gamma = \frac{(sen\phi - n)}{a\cos\phi}\left(\frac{-uy}{r} + \frac{vx}{r}\right) \tag{6}$$

Where n = 0.716, Ψ1 = 30°. For these cases, the true latitude is at 30° and 60° N.

As a regional model, it requires initial as well as lateral boundary conditions to run; this information was extracted from the US aviation gridded data (AVN model) covering the entire time integrated period.
The microphysics processes are parameterized (Grell et al., 1993) in:

a) Cumulus schemes, which represent sub-grid vertical fluxes and rainfall due convective clouds, producing column moisture, temperature tendencies and surface convective rainfall. In this system the Anthes-Kuo scheme where used.
b) Planetary boundary layer schemes, which represents sub-grid vertical fluxes due turbulence. Mostly distinguished by treatment of the unstable boundary layer. Provide column tendencies of heat moisture and momentum, interacts with fluxes from surface scheme and provides frictional effects on momentum. In this system the Bulk scheme where used.
c) Radiation schemes, which represent radiative effects in atmosphere and at surface, provides surface downwelling longwave and shortwave fluxes,

provides column temperature tendencies due to vertical radiative flux divergence. In this system the Simple Cooling scheme where used, with no diurnal dependence and is only a function of temperature.

d) Surface schemes, which represent effects of land and water surfaces, ground temperature based on heat budget using radiative fluxes and surface layer atmospheric properties, provides sensible and latent heat flux. In this system the Blackadar scheme where used.

3.2 WAVE MODELS

The wave models used in this study are discrete spectra and phase-averaged models (Battjes, 1994). The directional spectrum is resolved at each model grid point in terms of frequency-direction bands and the evolution of the wave field is found by numerically solving the spectral wave action (spectral energy equation in WAM) balance equation,

$$\frac{\partial N}{\partial t} + \nabla_{x,y} \cdot (\vec{c}_{x,y} N) + \nabla_{\sigma,\theta} \cdot (\vec{c}_{\sigma,\theta} N) = \frac{1}{\sigma}\left(S_{in} + S_{ds} + S_{nl} + S_{bf}\right) \qquad (7)$$

where N is the wave action spectrum, t is time, σ is the intrinsic angular frequency, θ is the wave direction, $c_{x,y}$ and $c_{\sigma,\theta}$ are the propagation velocities in physical and spectral domains. The left side of the equation represents the local rate of change of wave action density, propagation in physical space, and shifting of frequency and refraction due to the spatial variation of depth and current. The right side represents effects of wind input S_{in}, white-capping dissipation S_{ds}, nonlinear wave-wave interactions S_{nl} and bottom friction S_{bf}.

WAM is a third-generation wave model, which uses an explicit scheme to solve the wave energy transport equation, without *a priori* assumptions on the shape of the energy spectrum. The PROMISE version implemented here has additional features to allow it to run efficiently when applied to shallow water regions (Monbaliu *et al.* 2000). Wind input S_{in} and dissipation S_{ds} are based on the quasi-linear theory of wind-wave generation (Janssen 1989, 1991) following WAM cycle 4. Nonlinear interactions S_{nl} uses the discrete interaction approximation (DIA) of Hasselmann *et al.* (1985), and bottom friction S_{bf} follows Hasselman (1974), with additional mechanisms for dissipation by bottom friction and depth-induced wave breaking, as discussed by Monbaliu *et al.* (2000), Padilla-Hernández (2002), and Padilla-Hernández and Monbaliu (2003).

SWAN (Simulation of WAves in Nearshore areas) uses the action balance equation (7), with source terms for wind input S_{in}, nonlinear interactions (quadruplets S_{nl4} and triads S_{nl3}), whitecapping S_{ds}, bottom friction S_{bf} and

depth-induced wave-breaking S_{bk}. Documentation is given by Ris (1997), Booij *et al*. (1999), and Holtuijsen *et al.* (2003). Two different formulations can be used for S_{in}; one is based on Komen *et al.* (1984, 1994) as used in this study, and alternatively the other is based on Janssen (1989, 1991). The latter is in WAM cycle 4 and takes wave – wind interactions into account. DIA is used for S_{nl4}, and the Lumped Triad Approximation (LTA) from Eldeberky (1996), for nonlinear triad interactions S_{nl3}. SWAN has several S_{bf} expressions, from Hasselmann *et al.* (1973), Madsen *et al.* (1988) and Collins (1972), and S_{bk} follows Eldeberky and Battjes (1995) and Ris (1997).

4 WAVE MODEL VALIDATION

4.1 BATHYMETRY AND BUOY DATA

The operational wave prediction system uses the bathymetry Etopo2 v2 (2006), from the United States National Geophysical Data Center. This data base contains the world bathymetry with 2 minutes resolution, it was made combining data from several sources such as; echo sounder and gravity anomaly associated to the sea bottom obtained from altimeters mounted in satellites.

The bathymetric grid to be used by the models was extracted from the global one. The coarse grid (used by WAM) has a resolution of 1 degrees; it is shown in Figure 2, and the fine grid (used by SWAN) has a resolution of 0.1 degrees, shown in Figure 3, the characteristics of grids are shown in Table 1 and 2.

The wave measurements were obtained from buoys administered by the National Data Buoy Center (NDBC). In the Caribbean Sea there are three buoys (Figure 4), the closest one to Yucatan Peninsula is the buoy number 42056, located at 19.87^{o} N 85.06^{o} W. The buoy measure the following parameters: Air temperature and wind velocity (10 m above site elevation), atmospheric pressure, sea temperature (at 1m depth), the water depth in the site is 4446 m. (http://www.ndbc.noaa.gov/maps/West_Caribbean.shtml).

In order to validate the operational wave forecast system, statistical analysis is used to compare model results with observed data. The Root Mean Square Error (RMSE) is used to compare simulations against measured data. The root mean square error is defined as $rmse = \left[1/N \sum_i \left(y_i - x_i \right)^2 \right]^{1/2}$.

Where N is the number of data points, x_i the observations and y_i the model results.

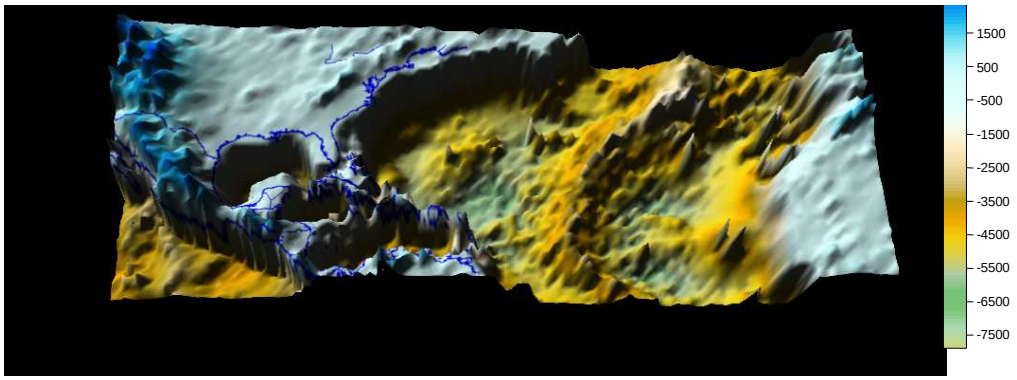

Figure 2. Coarse grid bathymetry with resolution of 1 degrees, extracted from the global data ETOPO 2.

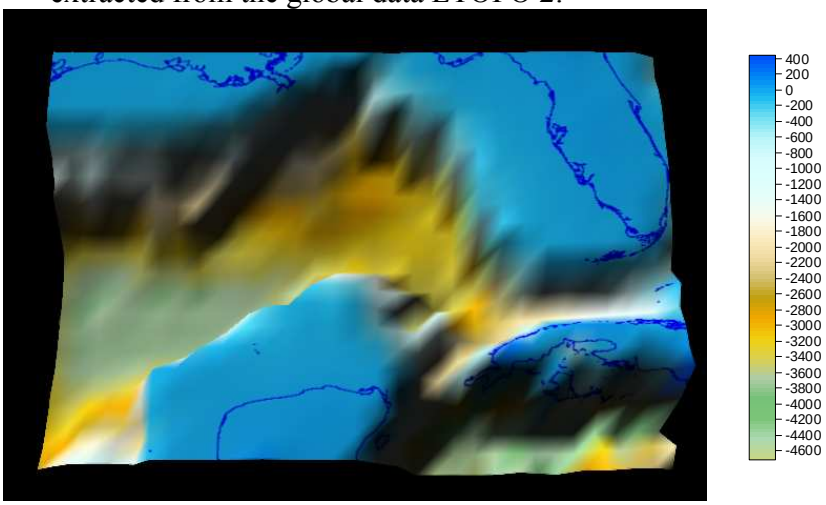

Figure 3. Fine grid bathymetry for the West Caribbean with resolution of 0.1 degrees, extracted from the global data ETOPO 2.

Table 1. Geographical location of the grids used in this study: $\Delta_{\lambda,\theta}$ is the resolutions in longitude λ and latitude ϕ, and $N\lambda$ and $N\phi$, are the number of points in λ and ϕ.

GRIDS	Longitude	Latitude	$\Delta_{\lambda,\theta}$	$N\lambda$	$N\phi$
Coarse (MM5)	-131º -7º	0.7º, 40º	0.25º	496	157
Coarse(WAM)	-98^{o} -20^{o}	$7^{o} - 31^{o}$	1^{o}	79	25
Fine (SWAN)	$-94^{o} - 82^{o}$	$18^{o} - 26^{o}$	0.1^{o}	121	81

Table 2. Spectral domains for wave models.

Parameters	Value
f_{low}, f_{high} [s^{-1}]	0.0412, 0.4060
nf , Δf	24, 0.1xf
nf , $\Delta\theta$	36, 10^{o}

Figure 4. Buoys location in the Caribbean Sea, (Taken from NDBC web page).

4.2 STUDY CASES

There have been selected three cases to evaluate the numerical models performance. The first case is a low energy situation, the second one is a cold front and the third one is the most extreme situations to evaluate the performance of atmospheric and wave models due to suddenly change of wind in direction and speed, a hurricane case.

a. Calm situation

The first case is a period of time when the atmosphere is in calm situation in the Caribbean Sea, the system was run for July 2007. The model results will be presented at the location of buoy 42056. Figures 5shows the time series of significant wave height (Hs), compared to the measured Hs. The modelled Hs peaks from SWAN are lower than the observed peaks, but achieve the appropriate timing. The underestimation of Hs reflects the possible wind underestimation by MM5 and/or the underestimation of boundary conditions by WAM. Model results for medium size wave (around 0.8m and 1.0 m) are the best approximating the measurements, while results in low wave conditions (smaller than 0.8m) are less good. The root mean square error (RMSE) for Hs is presented in Figure 6, for 12, 24, 36 and 48 hours. The smaller values for the RMSE are at 24 and 36 hours, the quality of forecast decreases at 48 hours, as expected.

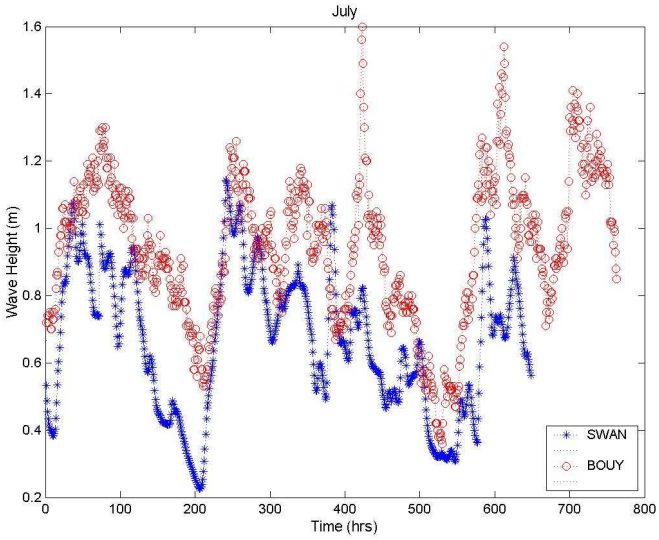

Figure 5. Significant wave height during the period of calm, July 2007.

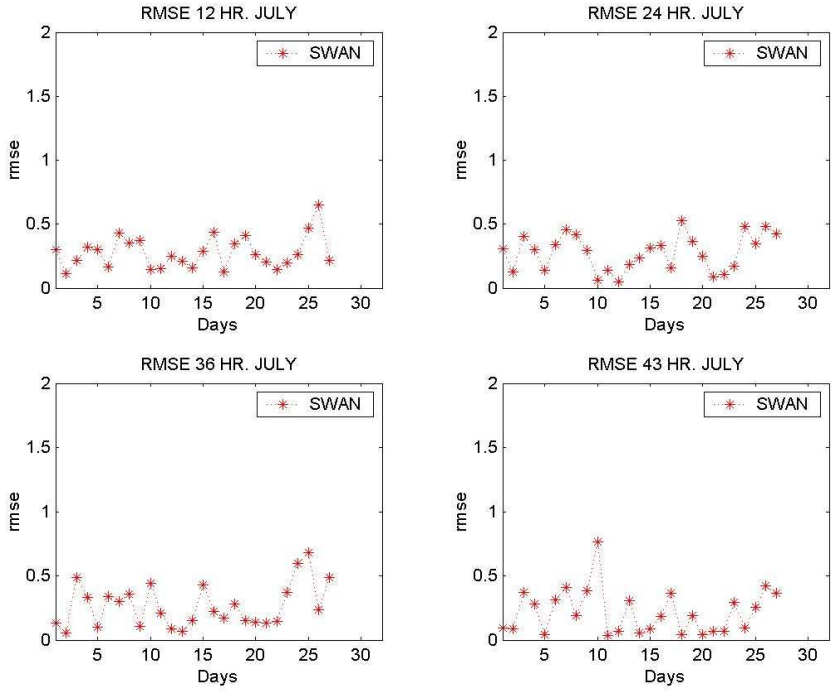

Figure 6. Root mean square of significant wave height taking the results at 12, 24, 36 and 48 hours forecast times.

b. Cold Front

At 0600 UTC 23 October, the Cold Front No. 4 (2007) was located in the Tamaulipas Mexican State, it moved south-westerly across the Mexican Coast, with

a surface pressure of 1042 hPa. with winds from 45 to 65 km/h and wind burst of 80 km/h. At 1800 UTC the cold front approached to Northern Veracruz State propagating cold mass to the eastern and center of Mexico. Over the Gulf of Mexico the wind burst reached 100 km/h. At 0000UTC 24 October, the cold front began to strengthen with wind burst of 120 km/h moving south-westerly to the Yucatan Peninsula across the Gulf of Mexico. From 25 to 26 October the cold front crossed the Gulf of Mexico, reaching a semi-stationary state on 27 October in the Eastern Gulf of Mexico, near the Yucatan Peninsula. The additional effects (precipitation) where registered in the south-eastern Mexico (Tabasco and Chiapas) at 1200 UTC 28 October, the local storms continued until 31 October in this area, with precipitation greater than 50 mm. At 1200 UTC, the system was located in the south- west Gulf of Mexico (Campeche Bay) maintaining stationary.

Cold fronts are meteorological events that have an important impact on the Gulf of México, and due to the fact that they produce strong winds with a small change in direction, they generate the highest waves in the south of Gulf of Mexico. They impede the navigation and they represent a real danger for oil rigs. The cold front No. 4 of the season 2007 (Figure 7) caused great impact in activities of PEMEX in the probe of Campeche; showing how important is to take into account wave forecast for decision makers. This front impacted the Gulf of Mexico from October 22 to October 27 2007. According to MM5, the maximum wind speed was 25 m/s, see Figure 8, where can be easily seen the consequent Tehuano wind (wind blowing through Tehuantepec region, reaching the Pacific Ocean) (Mexican Weather Service).

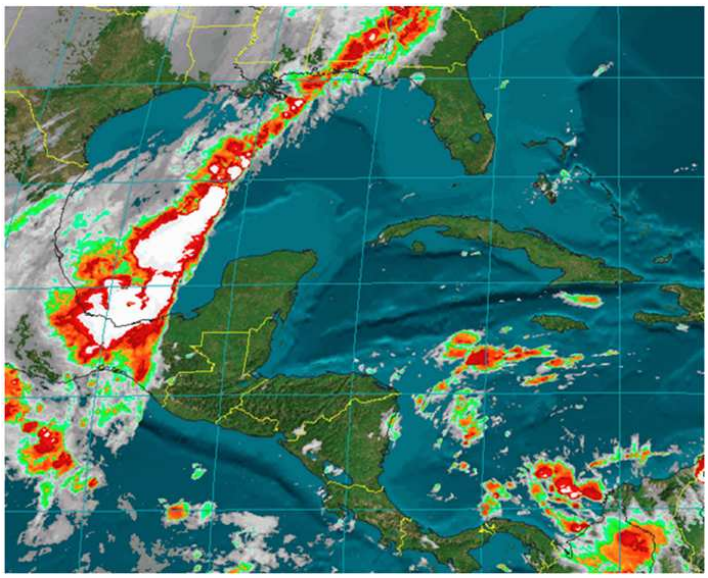

Figure 7. Post-processed satellite image of the cold front no. 4, 2007.

The cold front generated significant wave heights up to 6m at the most southern region of the gulf (Figure 9), unfortunately there are not wave measures on that region, but there are wave measurements from buoy 42056. Time series of

significant wave height, measured and modelled are shown in Figure 10. Simulated Hs follows the measurements, both time series exhibit two peaks at the maximum values of Hs, however the simulated Hs are lagged and underestimated by 25% approximately. In particular, for rapid wind speed increases, WAM responds more slow, and SWAN nested within WAM accentuates this slow response as stated in Padilla-Hernandez, et al. (2007).

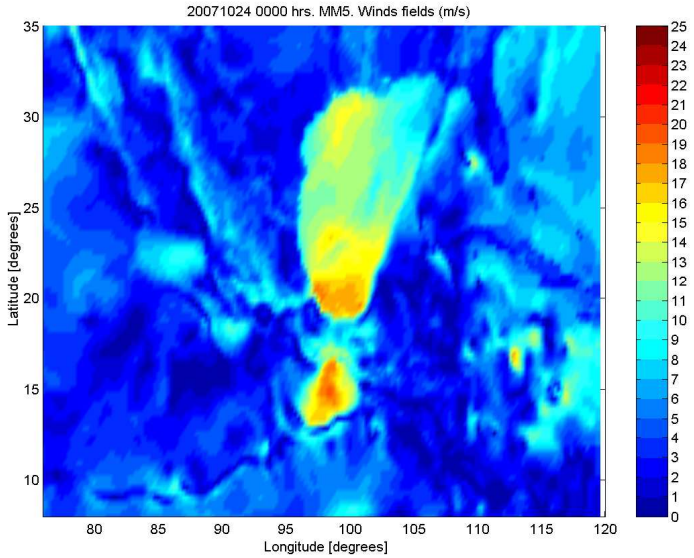

Figure 8. Numerical simulation of wind field by MM5 for the cold front no. 4 of 2007 season.

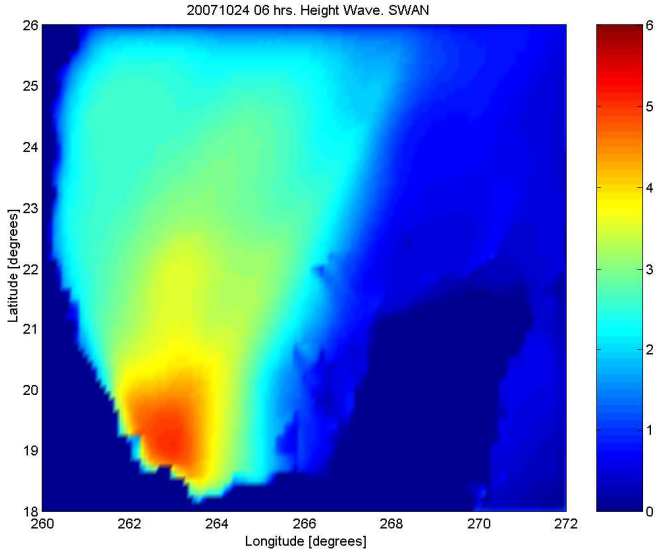

Figure 9 . Significant wave height field during the cold front

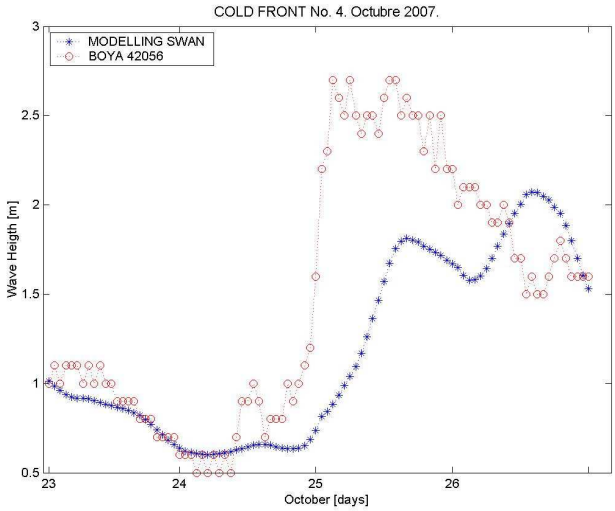

Figure 10. Significant wave height simulated, from buoy 42056, and modelled from SWAN, during the passage of the cold front.

c. Hurricane Dean

An extreme test for a wave forecasting system is a hurricane case due to the fast change in wind speed and direction. During the passage of Hurricane Dean, The POMA system was working operationally. Hurricane Dean was originated from an easterly wave that crossed the Atlantic coast of Africa on 11 August 2007. At 0600 UTC 13 August, Dean was considered a tropical depression in the Eastern Atlantic. The depression moved westward at about 36 km/h., at 1200 UTC 14 August,. On 16 August, Dean became a hurricane, with an intensity of 144 km/h by 1200 UTC. Dean entered the Caribbean Sea on 17 August around 0930 UTC, then began to strengthen rapidly in the eastern Caribbean, its winds increasing from category 1 to category 5 on the Saffir-Simpson Hurricane Scale in the 24 h ending at 0600 UTC 18 August with a minimum central pressure of 923 hPa.

Dean began to strengthen as it approached the Yucatan Peninsula. As the eyewall contracted, Dean regained Category 5 status near 0000 UTC 21 August, the center made landfall in the Yucatán Peninsula near 0830 UTC, with a minimum central pressure of 905 hPa and maximum sustained winds of 270 km/h. Dean weakened as it moved across the Yucatan Peninsula, emerging into the Bay of Campeche around 1900 UTC. Dean maintained hurricane strength throughout its 10-h passage over land. Deep-layer high pressure along the northern coast of the Gulf of Mexico kept Dean on its west-northwestward track until 1200 UTC 22 August, when the cyclone turned to the west. Dean made landfall again at 1630 UTC that day near Tecolutla, Veracruz, Mexico, as a Category 2 hurricane with winds of 153 km/h. Dean weakened rapidly after landfall, becoming a depression by 0000 UTC 23 August, and dissipating over the mountains of central Mexico shortly thereafter (National Hurricane center)

Figures 12 and 13 show the relative size and the track of Hurricane Dean respectively (from NOAA). MM5 model located the hurricane center adequately; however the wind intensity was underestimated and consequently there is an underestimation of Hs. Figure 14 shows the time series wind speed at location of buoy 42056. The underestimation of wind speed is about 20% at peak, giving values of modelled Hs, at the peak, 50% lower than measured Hs. MM5 achieves the appropriate timing during the peak of wind intensity, occurring at the same time as the observed peak.

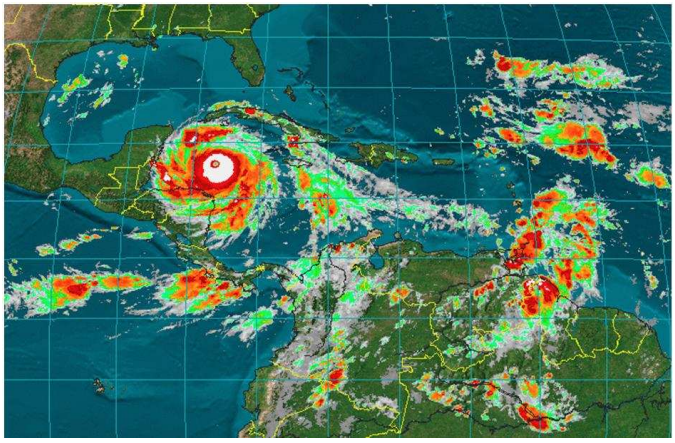

Figure 12. Satellite image of Hurricane Dean, August 2007

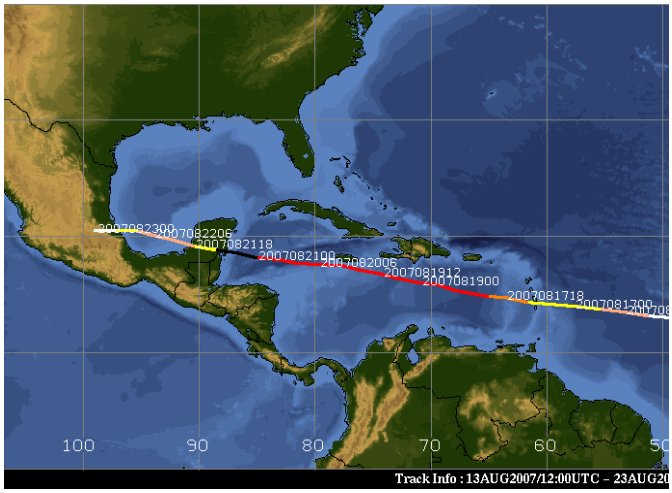

Figure 13. Hurricane Dean track, August 2007

Figure 15 shows the time series of measured and modelled Hs from SWAN at location of buoy 42056. Except during the peak, Hs from SWAN approach the measurements very well. As MM5, SWAN achieves the appropriate timing, as well, during the Hs peak, occurring at the same time as the measured Hs peak.

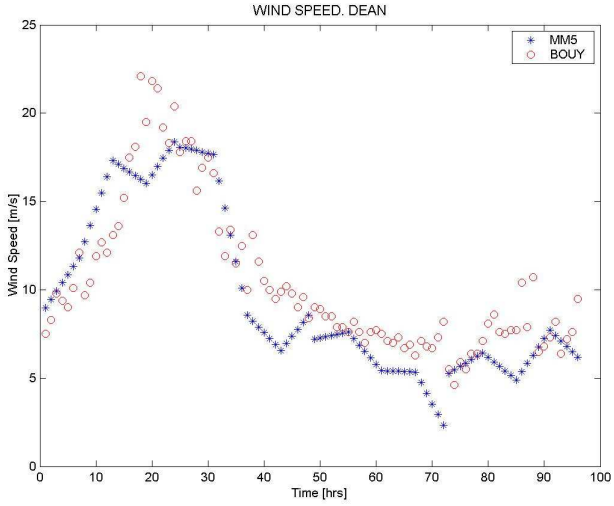

Figure 14. MM5 wind speed, as implemented in the two wave models, compared to measured winds at buoy 42056

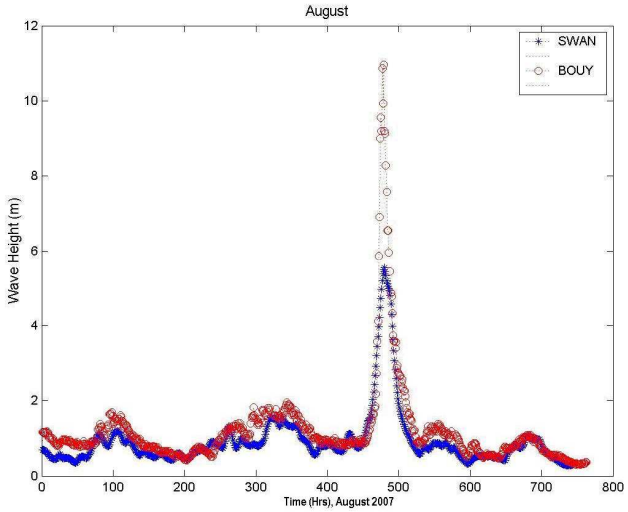

Figure 15. Time series of measured and modelled results from SWAN for Hs, at location of buoy 42056, for Hurricane Dean.

Being identified the wind speed underestimation, an exercise incrementing the wind speed in 25% during the maximum wind intensity in the whole domain, to see how SWAN performs using winds closer to the wind measurements. The new wind time series is shown in Figure 16. The time interval limited by the vertical lines represents the time when the wind has suffered an increment. The computed Hs using the new wind are shown in Figure 17. The modelled Hs peak from SWAN is now very close of the observed peak. This can be observed in the RMSE for the original results and for the new Hs using the increased wind speed.

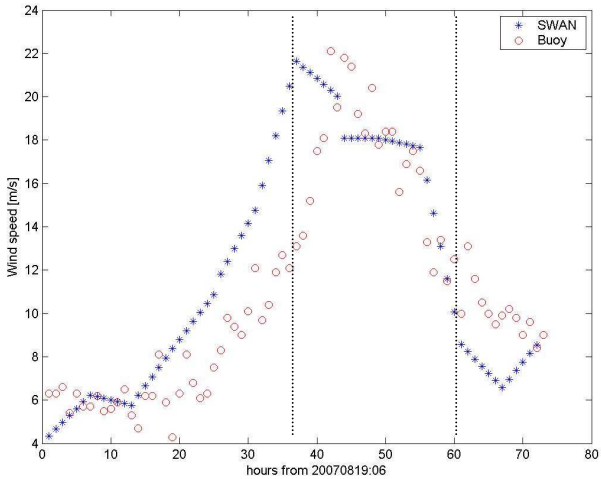

Figure 16 Time series of wind Speedy incremented 25% Turing the interval between the two vertical lines, 24 hours.

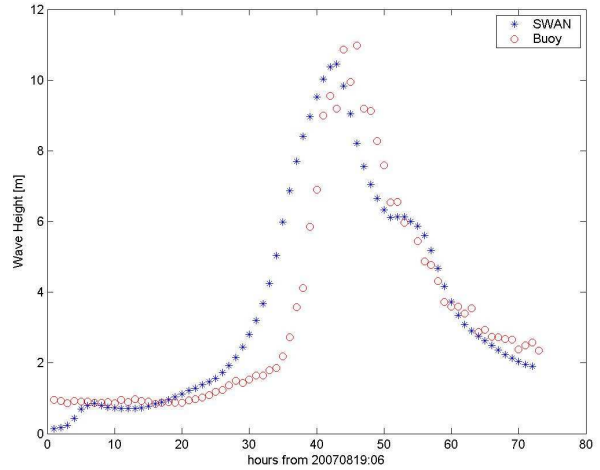

Figure 17. Time series of measured and modelled Hs from SWAN using the modified wind.

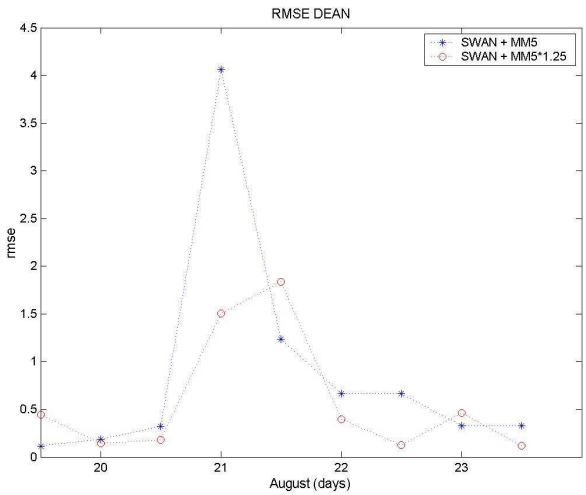

Figure 18. RMSE for Hs using the original wind from MM5 (stars) and the modified wind increased 25% (circles).

5. CONCLUSIONS

The wind-wave forecasting system is working in an operational way in a five domains in a nested fashion over the Mexican waters: Caribbean grid , east of Gulf of México, west of Gulf of Mexico, south of Mexican Pacific and on the west coast of Mexico. In this paper, the results for the Caribbean grid are presented.
As described above, the POMA system underestimates wind speed mainly during the peak of extreme events, such as the cold front and the hurricane cases, presented in this paper. It is believed that simulation of Hs will be better with the introduction of wind fields every hour from MM5, instead of every 6 hours, as it was done during the events presented. This will improve the forecasting mainly during extreme events such as fronts, tropical storms and hurricanes where wind direction and speed changes drastically in a short period of time and in a short distance. Validation of POMA system is in progress.

Future work
It is necessary to validate the forecasting system, the atmospheric model MM5 and both wave models, WAM and SWAN. It will be done for more cases of hurricanes and fronts, forcing the wave models using hourly wind fields.
To analyze the Hs, peak period, frequency and directional spectra.
Set up the system on domains which are useful for the final users, such as, PEMEX, CFE, IMT and other Mexican institutions.
To couple the wind and wave models to an oceanic circulation model, to take into account the wave currents interactions, mainly in coastal regions.
To plan an adequate commercialization scheme, to attend diverse clients in Mexico and Latin America by means of the service of numerical simulation giving them access through a web page hosted in IMTA.

References.

Battjes, J.A., 1994: Shallow water wave modelling. Proc. Int. Symp. Waves -Phys. Numerical Modelling. University of British Columbia, Vancouver, I, 1-23.

Booij, N, R.C. Ris, and L. H. Holthuijsen, 1999: A third-generation wave model for coastal regions. 1. Model description and validation. J. Geophys. Res., 104 (C4), 7649-7666.

Collins, J.I., 1972: Prediction of shallow water spectra. J. Geophys. Res., 93 (C1), 491-508.

Dudhia, J., 1993: A nonhydrostatic version of the Penn State/NCAR mesoscale model: Validation tests and simulation of an Atlantic cyclone and cold front. Mon. Wea. Rev., 121, 1493-1513.

Eldeberky, Y., and J.A. Battjes, 1996: Spectral modelling of wave breaking: Application to Boussinesq equations. J. Geophys. Res., 101 (C1), 1253-1264.

Grell, G., 1993: Prognostic evaluation of assumptions used by cumulus parameterizations. Mon. Wea. Rev., 121, 764-787.

Hasselmann, K., 1974: On the spectral dissipation of ocean waves due to whitecapping. Bound.-Layer Meteor., 6, 107-127.

Hasselmann, K., T.P. Barnett, E. Bouws, H. Carlson, D.E. Cartwright, K. Enke, J.I. Ewing, H. Gienapp, D.E. Hasselmann, P. Kruseman, A. Meerbrug, P. Müller, D.J. Olbers, K. Richter, W. Sell, and H. Walden, 1973: Measurements of wind-wave growth and swell decay during the Joint North Sea Wave Project (JONSWAP). Dtsch. Hydrogr. Z., A8(12), 95 pp.

Hasselmann, S., K. Hasselmann, J.H. Allender. and T.P. Barnett, 1985: Computations and parameterizations of the nonlinear energy transfer in a gravity-wave spectrum. Part. II: parameterizations of the nonlinear energy transfer for application in wave models J. Phys. Oceanogr., 15, 1378-1391.

Holthuijsen, L.H., N. Booij, R.C. Ris, IJ. G. Haagsma, A.T.M.M. Kieftenburg, E.E. Kriezi, and M. Zijlema, 2003: SWAN Cycle III version 30.20. User Manual. Delft University of Technology, The Netherlands.

Janssen, P.A.E.M., 1989: Wave-induced stress and the drag of the air flow over sea waves. J. Phys. Oceanogr., 19, 745-754.

Janssen, P.A.E.M., 1991: Quasi-linear theory of wind-wave generation applied to wave forecasting. J. Phys. Oceanogr., 21, 1631-1642.

Komen, G.J., S. Hasselmann, and K. Hasselmann, 1984: On the existence of a fully developed wind-sea spectrum. J. Phys. Oceanogr., 14, 1271-1285.

Komen, G. J., L.Cavaleri, M. Donelan, M. Hasselmann, S. Hasselmann, P. A. E. M. Janssen, 1994: Dynamics and Modeling of Ocean Waves. Cambridge University press, 520pp.

Madsen, O.S., Y.-K. Poon, and H.C. Graber, 1988: Spectral wave attenuation by bottom friction: theory. Proc. 21st Int. Conf. Coastal Eng., ASCE, 492-504.

Monbaliu, J., R. Padilla-Hernández, J.C. Hargreaves, J.-C. Carretero, W. Luo, M. Sclavo, and H. Günther, 2000: The spectral wave model WAM adapted for applications with high spatial resolution. Coastal Eng., 41, 41-62.

Padilla-Hernández, R., 2002: Numerical modelling of wind wave energy dissipation at the bottom including ambient currents. Ph.D. dissertation, Katholieke Universiteit Leuven, Belgium, 171 pp.

Padilla-Hernández, R., and J. Monbaliu, 2003: WAM-PROMISE, Extension 1. Internal Report. Hydraulics Laboratory, Katholieke Universiteit Leuven, Belgium.

Ris R.C., 1997: Spectral modelling of wind waves in coastal areas. Ph.D. dissertation. Delft University of Technology, The Netherlands, 160 pp.

SWAN Cycle III version 40.20, 2003. User Manual. Holthuijsen. L, Booij N, Ris R.C., Haagsma I.J. Delft University of Technology.

WAMDI group, 1988: The WAM model – a third generation ocean wave prediction model. J. Phys. Oceanogr., 18, 1775-1810.

WAM-PROMISE extension 1 manual. 2002. Padilla-Hernández, R., Monbaliu J. Laboratorium voor Hidráulica K.U. Leuven.